Published in final edited form as:
Brain Res. 2009 November 3; 1296: 225–233. doi:10.1016/j.brainres.2009.06.101.

A Nerve Model of Greatly Increased Energy-Efficiency and Encoding Flexibility over the Hodgkin-Huxley Model

Jurgen F. Fohlmeister
Department of Integrative Biology and Physiology University of Minnesota

Abstract

A mammalian "RGC model" (retinal ganglion cells) is distinguished from the Hodgkin-Huxley model by the virtual absence of K-current *during*, and the virtual absence of Na-current *after*, the regenerative (rising) phase of the action potential. Both Na- and K-currents remain negligible throughout the interspike interval, whose control is therefore relinquished to stimulus currents. These properties yield a highly flexible and energy-efficient nerve impulse encoder. For the Hodgkin-Huxley model, in contrast, only 15 % of the Na-ions enter the axon regeneratively during the action potential (squid giant axon); a wasteful 85 % enter during the falling phase. Further, early activation of K-current causes the Na- and K-currents of the action potential to dominate over stimulus currents in controlling the sub-threshold membrane potential (interspike interval). This property makes the Hodgkin-Huxley model an intractable high frequency oscillator, which *cannot* be converted to flexible impulse encoding. The temperature difference between the squid giant axon (6.3° C) and RGCs (37° C) is bridged by a Q10 analysis, which suggests that an additional molecular gating mechanism of high Q10 – which is not present in the squid – is active in RGCs.

Keywords

Ion Channel Gating; Nerve Action Potential Encoder; Energy Efficient; Hodgkin-Huxley Model; Temperature Q10

1. INTRODUCTION

The demands placed on a nerve axon are simple and all-or-none; i.e., to faithfully pass on (*propagate*) all approaching action potentials and, equally important, to otherwise remain silent. In contrast, the encoding of nerve impulses can be a delicate process of *creating* highly variable signals in response to a wide range of stimuli. The requirements of these two purposes are contradictory, in that faithful propagation is best assured with a high threshold for the action potentials (i.e., electrical stability) which, however, prevents the necessary sensitivity for flexible impulse-encoding. The Hodgkin-Huxley model satisfies the stability requirement, but violates that of flexibility, even when its impulse-threshold is lowered by increasing the sodium conductance, G_{Na}.

Contact Information: Dr. J. F. Fohlmeister, Department of Integrative Biology and Physiology, 6-125 Jackson Hall, 321 Church street S.E., University of Minnesota, Minneapolis, MN 55455, Telephone: (612)-625-6958, FAX: (612)-625-5149, E-mail: jurgen@umn.edu.

The Hodgkin-Huxley model has been remarkably durable, in part because of its mathematical elegance (simplicity and transparency), and in part because its gating kinetic rate constants reproduce the action potential waveform (roughly triangular), and *large* ionic membrane currents of the squid giant axon remarkably well (*Loligo pealei*, *L. vulgaris*). However, many action potentials of mammalian central neurons are of a more rounded waveform, associated with significantly smaller membrane ion-currents (cf Attwell and Laughlin, 2001). In a comparative model developed for retinal ganglion cells ("RGC model"), these features arise exclusively from the temporal relationships and relative voltage-dependence among the gating rate constants of the regenerative Na- and delayed rectifier K-channels. Although the RGC model shares the underlying gating-kinetic *structure* of Hodgkin and Huxley (1952), including the property of a "quasi-threshold" for action potentials (coined by FitzHugh, 1955), functionally the two models differ fundamentally. It is shown here that flexibility in impulse encoding is directly related to the efficient use of the energy that drives the ionic currents, that optimizing the efficiency yields the greatest flexibility, and both efficiency and flexibility are inversely related to the magnitudes of the Na- and K-currents that are minimally necessary to generate action potentials in the face of membrane capacitance.

2. RESULTS

The RGC model as an energy-efficient and flexible nerve impulse encoder

The steady state fraction of open activation gates in the RGC model is – for *all* membrane potentials – smaller for K-channels than for Na-channels (i.e., for all V, $n_\infty^4(V) < m_\infty^3(V)$; see Figure 1B). Thus the K-current of the RGC model becomes substantially activated only *after* the threshold for an action potential is crossed. This contrasts with the Hodgkin-Huxley model (see below), and reflects a relative voltage-shift in the rate constants $\alpha_n(V)$ and $\beta_n(V)$, so that similar levels of K-channel activation occur 13 mV more depolarized in the RGC model (rate constants are listed in Computational Procedure).

There is, in addition, a significantly greater difference between the overall *rate* of Na-gating and the overall *rate* of K-gating in the RGC model, than for the Hodgkin-Huxley model (underlined coefficients of the listed rate constants, and Fig. 1C). Therefore, Na-*in*activation is nearly complete by the time of onset of significant K-activation gating in an RGC model action potential. The resulting virtual absence of K-current throughout the regenerative phase, and the virtual absence of Na-current throughout the falling phase of the action potential (Fig. 1A, Fig 2A), make the RGC model highly energy-efficient, in the sense of minimizing the ionic currents.

After the K-channels close in afterhyperpolarization, the virtual absence of *both* primary currents, I_{Na} and I_K, continues throughout the interspike interval of the RGC model. Thus the sub-threshold membrane potential "drifts easily" and – unlike the Hodgkin-Huxley model – responds exclusively to small or large stimulus currents (synaptic or injected). This is the essence of flexible impulse encoding, which yields a large dynamic range of impulse-frequencies, including very low frequency repetitive firing (see Discussion). The RGC model rests close to its leakage reversal potential, which is arbitrary within a wide range (~ − 75 to − 55 mV).

Contrasting properties of the Hodgkin-Huxley model: An energy-*in*efficient high frequency oscillator

A prominent feature of the Hodgkin-Huxley model is that its *peak* of sodium current occurs *after* the peak of the action potential, a period during which the sodium current of the RGC model is virtually zero (Fig. 2A). Thus, for the Hodgkin-Huxley model, 85 % of the Na-ions that enter the axon during an action potential do so *after* the regenerative phase (Fig. 2B).

Although this percentage is reduced to 68 % at 37° C, the late and large I_{Na} flows in direct opposition to the (therefore *necessarily*) large I_K throughout the repolarizing phase. This rate constant-imposed competition between the ionic currents I_{Na} and I_K makes the Hodgkin-Huxley model highly wasteful of the energy used by the ionic currents.

Note that in the Hodgkin-Huxley model, $n_\infty^4(V) > m_\infty^3(V)$ throughout the range of $V < -28$ mV (Fig. 1B). Thus, unlike the RGC model, the K-channels begin to substantially activate *prior* to reaching the subsequent impulse-threshold in repetitive firing. This causes the (sub-threshold) interspike trajectory of the Hodgkin-Huxley model to be controlled primarily by the rate constants of gating, I_{Na} and I_K, just as these control the waveform-trajectory of the action potential, and both trajectories are relatively weak functions of stimulus current.

This gating-kinetic control of the interspike trajectory is unrelated to the high threshold of the Hodgkin-Huxley model. That threshold can be reduced, or entirely eliminated, by unilaterally increasing the sodium current (i.e., increasing G_{Na}, listed in Computational Procedure). The model becomes spontaneously firing (stimulus = 0) when G_{Na} is increased by a factor of about 1.8. Despite these threshold-changes, the length of the interspike interval is – in all cases – constrained by the rate constants of I_{Na} and I_K; the maximum length (minimum impulse frequency) is absolutely restricted, and large stimulus currents are required to reduce the length of the interspike interval. It is this ubiquitous gating-kinetic control that makes the Hodgkin-Huxley model an intractable high frequency oscillator, and therefore incapable of flexible impulse-encoding (cf. also Fohlmeister et al., 1980).

Coordination among the channel-gating processes; Capacitive “smoothing”

When membrane capacitance is zero ($C_M = 0$), the ionic conductances can be reduced almost to zero (maintaining the model-specific ratios of G_{Na}: G_K), and both models continue to generate “zero-C” (i.e., purely conductive) action potentials of full amplitude. Thus, in the absence of capacitive current ($I_C = C_M\, dV/dt = 0$), the gating kinetics alone, with arbitrarily small (or large) G_{Na} and G_K, yield the appropriate *sequential timing* of Na- and K-activation and Na-inactivation to generate the $I_{Na}(t)$ and $I_K(t)$ necessary for an action potential.

In the presence of membrane capacitance, conservation of current (Kirchoff’s law) requires that the sum $I_C + I_{Na} + I_K = 0$ (apart from stimulus, leakage, and other negligible currents). In the RGC model, $I_{Na} + I_K \sim I_{Na}$ during the regenerative phase, and $I_{Na} + I_K \sim I_K$ during the falling phase of the action potential (where Ca-current also contributes; see Fig. 1A). Because I_K is small during the rising phase and I_{Na} is small during the falling phase, each of these two currents is comparable to I_C during their respective phases, and this implies substantial capacitive effects.

These capacitive effects reduce dV/dt (capacitive “smoothing”). This alters the temporal voltage profile to which the gating rate constants respond, which can change the sequential timing among the several channel gating processes. Figure 3 shows that for the RGC model, the temporal duration (width) of the “capacitive” action potential is greater than the width of the zero-C action potential by factors of about 2 (at mid-amplitude) or 3 (impulse-threshold to afterhyperpolarization). The ability of the RGC model to generate both capacitive and zero-C action potentials with this degree of difference in voltage profile implies that the gating rate constants of I_{Na} and I_K *coordinate* the separate rising and falling phases. Further, because the ionic conductances, G_{Na} and G_K, change with temperature at the specific rate of Q10 = 1.47, these same factors (about 2 or 3) hold at every temperature from 6.3° to 37° C (Fig. 3). (Q10 < 1.47 would cause to increase these factors with increasing temperature; Q10 > 1.47 would cause to reduce them.) Thus the gating coordination of the RGC model over different temperatures is not much influenced by capacitance.

For the Hodgkin-Huxley model, in contrast, the gating of I_{Na} and I_K is *not* coordinated into separate rising and falling phases for the action potential. The primary reason is that both Na- and K-activation are closely linked to the rising phase, and capacitive loading will change their relative timing, which can cause impulse-failure. For this reason, I_{Na} and I_K are both large in comparison with I_C. The broad current maxima during an action potential [threshold-shock induced] reach $I_{Na} = -767.7\ \mu A/cm^2$, $I_K = 801.8\ \mu A/cm^2$, and $I_C = -68.2\ \mu A/cm^2$ with a brief early peak of $I_C = 214.8\ \mu A/cm^2$ (cf Fig. 2A). This comparatively small I_C yields little capacitive smoothing, and therefore the capacitive and zero-C action potentials of the Hodgkin-Huxley model are of nearly the same duration (width) at any given temperature (see Fig. 3).

Calcium current

The high threshold (H-type) Ca-current of the RGC model increases the peak amplitude of the action potential by several millivolts, and reshapes the falling phase. Because of the resulting increased depth of afterhyperpolarization, the presence of I_{Ca} also somewhat reduces the impulse frequency in repetitive firing (Fohlmeister and Miller, 1997a). However, because the flow of H-type Ca-current is virtually zero *throughout* the interspike interval, removing the Ca-channel has no effect on the RGC model's flexible encoder properties. For the same reason, adding a Ca-current to the Hodgkin-Huxley model (in the RGC ratio of G_{Ca}: $G_{Na} = 0.0275$, see [*] in Computational Procedure), has no effect on that model's rigid oscillator characteristic (see Discussion).

Differential thermal behaviors of the squid giant axon and retinal ganglion cells

In bridging the temperature span between the standard 6.3° C of the Hodgkin-Huxley model, and the mammalian 37° C of the RGC model, the following features were found (the 'matches' in [1, 2] are in the *durations* of the action potentials):

1. Starting at 6.3° C, the gating kinetic Q10 = 2 applied to the Hodgkin-Huxley model yields 'matched' action potentials with the RGC model (and with retinal ganglion cells) throughout the temperature range of T > 23° C (Fig. 4A [open diamonds connected by horizontal small dots], and Fig. 3 [heavy curves for 37° C]).
2. Starting at 37° C, the *same* gating kinetic Q10 = 2 applied to the RGC model yields an action potential 'match' with the Hodgkin-Huxley model (and with the squid giant axon) at 6.3° C (Fig. 3 [heavy curves for 6.3° C]).
3. *Experimentally* for retinal ganglion cells, uniformly constant Q10s = 1.95 (Na-gating) or 1.9 (K-gating) were previously found for the partial temperature range of T > 23° C (Fohlmeister et al., 2009). For lower temperatures, the experimental gating kinetic Q10 increases for RGCs, and reaches Q10 = 8 at about 10° C (Fig. 4A [large dots]).

To relate [2] and [3], note that the action potential of the 6.3° C squid axon (and Hodgkin-Huxley model) is about 2.5 milliseconds in duration. For retinal ganglion cells, in contrast, the duration of action potentials at the *lowest* temperatures (7° to 8° C) is about 10 milliseconds (Fig. 4D). Thus, the *empirical* impulse 'match' with the 6.3° C squid axon occurs for RGC *data* at 13.9° C. Indeed, retinal ganglion cells do not generate action potentials at 6.3° C.

Regarding [3], the combination of a substantial temperature range of uniformly *constant* Q10, and a neighboring *lower* temperature range of increasing Q10, is consistent with two simultaneously active processes in RGC gating, whereby the process of constant Q10 is rate-limiting at high temperatures, and a second process (of high Q10) becomes rate-limiting at low temperatures (see Discussion). A distinct second process is specifically suggested for RGC gating, because of its apparent absence in the squid axon:

Thus, in order to match the relatively short action potential duration of the 6.3° C squid axon, the gating kinetic Q10 = 2 is *flat* across the *full* temperature range (6.3° to 37° C) [1, 2]. A *flat* Q10 suggests a simpler gating mechanism for the squid axon. The similarity between the *flat* Q10 (= 2), and the *partial* range *constant* Q10s (= 1.95, 1.9) of RGC gating, suggests that this simpler gating mechanism is the *same* process in both preparations. Being conserved across the species, this process may represent the irreducible minimum mechanism necessary for Na- and K-channel gating in general, to which other processes of high Q10 appear to be added in mammalian channel gating. Further details are given in Discussion.

3. DISCUSSION

Flexible impulse encoding requires that stimulus currents (synaptic or injected) have a “free hand” in moving the sub-threshold membrane potential, without interference from the effects of voltage-gating of the Na- and K-currents of the action potential (cf Fourcaud-Trocme et al., 2003; van Rossum et al, 2003). This condition is inherently satisfied by the RGC model rate constants, which simultaneously optimize the gating kinetics metabolically. Thus the functionally needless, and therefore wasteful fraction of 85 % of Na-ions (and balancing K-ions) that cross the membrane during the action potential of the Hodgkin-Huxley model, is reduced to virtually zero in the RGC model (Fig. 1A, Fig 2A). The metabolic energy demand for Na-K-ATPase ion pumping is thereby reduced by a *factor* of nearly eight (7.76 in Fig. 2B; cf Attwell and Laughlin, 2001). The associated reduced membrane conductances also lower the necessary number of channel molecules (channel density) by a *factor* of nearly six (cf Naundorf et al., 2006). Thus, the primary conclusion of the present comparative results is that the elegant framework and mathematical simplicity of the Hodgkin-Huxley model may well be employed in simulating encoder-excitation of mammalian neurons, *provided appropriately modified rate constants are used*.

The RGC model rate constants; ‘Sleepy’ Na-channels

The RGC model rate constants involve two types of modification relative to Hodgkin and Huxley (1952): [1] Voltage-shifts, and [2] changes in the overall gating rates. Voltage-shifts apply primarily to K-channel gating (also Na-inactivation; cf Fig. 1B); changes in the overall gating rates to Na-channels (see listed rate constants in Computational Procedure). Na-channel gating is significantly faster in the RGC model, which separates and coordinates the ionic currents I_{Na} and I_{K} in the rising and falling phases of the action potential (see Results). The voltage-shifts suppress the early K-channel activation of the Hodgkin-Huxley model, in that they cause to require a greater depolarization for equivalent K-channel gating.

In a remarkable empirical coincidence it was found that the voltage-shifts *alone* are not sufficient to yield either the efficiency or the flexibility properties of the RGC model. Thus, Figure 4B shows an experimental impulse train from a rat RGC, with “sleepy” Na-channels. The impulse train was generated in response to a just over threshold constant stimulus current, at 8° C (data courtesy of Eric A. Newman). Note the (sporadic) spiking, in conjunction with sub-threshold oscillations that are characteristic of the Hodgkin-Huxley model (see below); note also the Hodgkin-Huxley-like shape of the interspike trajectory (expanded in Fig. 4C). Precision fitting (phase plots) of the experimental action potentials – which took full account of the non-space clamped nature of the experimental recording – showed that the Na-channels of rat RGCs consistently become “sleepy” for $T \leq 8°$ C, while the K-channels remain *non*-sleepy (Fohlmeister et al., 2009). The modeling showed that “sleepy” Na-channels *retain the voltage-shifts of the RGC model*, but their gating is slowed by a factor of about 10.

The modeling showed further that “sleepy” Na-channels induce a competitive overlap of I_{Na} and I_{K}, and cause the peak of I_{Na} to occur during the falling phase in “sleepy action potentials,” with 74.7 % of Na^{+} ions entering the cell after the peak of the action potential (see

Figure 9 in Fohlmeister et al., 2009). Except for the sporadic nature of the spiking – which may be due to channel or synaptic noise in this just over threshold recording – these phenomena are characteristics of the Hodgkin-Huxley model (Fig. 2A). The peak currents during the action potential are $I_{Na} = -31\ \mu A/cm^2$, $I_K = 36\ \mu A/cm^2$, and $I_C = 7.5\ \mu A/cm^2$, whose relative proportions, and the ionic currents' dominance over I_C, are again like those of the Hodgkin-Huxley model (see Results). For this reason too, there is little capacitive smoothing of the "sleepy action potentials," which are of about 10 ms duration (Fig. 4D).

Repetitive Firing; Ca-activated K-current, and Electrotonic current

When the currents of the action potential, I_{Na} and I_K, are coordinated as they are in the RGC model, the impulse frequency (in repetitive firing) is determined by external stimulus in conjunction with (typically small) intrinsic neural currents. Thus, it was previously found with morphologically reconstructed model neurons, that the electrotonic current (in the encoder region of the neuron) can significantly reduce the impulse frequencies generated by small stimulus currents (Fohlmeister and Miller, 1997b; Fohlmeister et al., 2009). It was also found that the Ca-activated K-current, $I_{K(Ca)}$, can similarly reduce the impulse frequencies in space clamped (single compartment) simulations (Fohlmeister and Miller, 1997a).

The top traces of Figure 5 show an impulse train of the space clamped RGC model (which implicitly includes $I_{K(Ca)}$) at 37° C. The low frequency segments of that impulse train (< 2 impulses / sec) are interrupted by two periods of larger stimuli, and the three resulting impulse frequencies fall on a nearly linear F/I curve (frequency-versus-stimulus; see Fig. 5 caption), and also show that the RGC model is fully capable of generating and following very high impulse frequencies (> 1,000 impulses / sec, at 37° C).

The center traces of Figure 5 show two superposed impulse trains generated by the Hodgkin-Huxley model at 37° C, with $I_{STIM} = 21\ \mu A/cm^2$ (dashed curve; which does *not* sustain repetitive firing), and $I_{STIM} = 21.5\ \mu A/cm^2$, which does yield steady-state repetitive firing near the lowest model-attainable impulse frequency (~ 360 impulses/sec, at 37° C). The exclusion of lower frequencies lies in the model's gating rate constants, *not* in the high threshold-stimulus, which can be reduced by increasing the sodium conductance, G_{Na} (see Results). To introduce some encoding flexibility into the Hodgkin-Huxley model, therefore, requires an added mechanism to delay the onset of activation gating of I_K and I_{Na} in the interspike interval.

This was done in the bottom traces of Figure 5, for which $I_{K(Ca)}$ was added the Hodgkin-Huxley model (also I_{Ca} to activate the $I_{K(Ca)}$). The threshold of this compound model was also reduced to just above spontaneous firing (see Fig. 5 caption); this was necessary because the relatively small $I_{K(Ca)}$ becomes functionally ineffective with large I_{STIM}. Thus, the low frequency segments of the impulse train were generated with the relatively small $I_{STIM} = 2\ \mu A/cm^2$.

Note that when the stimulus is increased to $I_{STIM} = 6\ \mu A/cm^2$, the individual action potentials of the impulse train become replaced by impulse-doublets (bottom left record of Fig. 5, segment 0.3 – 0.5 sec). As I_{STIM} is further increased, the impulse-doublets are replaced by damped impulse-bursts (of the type seen in the dashed record immediately above). The impulse-bursts coalesce and convert to continuous high frequency firing when I_{STIM} reaches $8\ \mu A/cm^2$ (record segment of 0.775 – 0.85 sec). Thus the F/I curve of this compound Hodgkin-Huxley model includes a substantial range of low impulse frequencies (for $I_{STIM} < 6\ \mu A/cm^2$), followed by a relatively rapid transition to the very high frequency firing characteristic of the Hodgkin-Huxley model.

This type of encoding "flexibility" may be appropriate to the head of the squid giant axon (a motor neuron), one of whose primary purposes is to induce strong and rapid mantle-contraction, resulting in escape motion, a "flight response." The range of low impulse frequencies could serve to modulate the muscle tonus of the resting mantle, which then readily converts to high frequency impulse activity when necessary for "flight."

Note that a kind of 'ringing' (high frequency oscillation) precedes the action potentials in low frequency firing by the compound Hodgkin-Huxley model (seen most clearly in the bottom-right records of Fig. 5). This 'ringing' (of *increasing* amplitude) occurs with any slowly and smoothly increasing stimulus current ('ramp stimulus') as the threshold of the Hodgkin-Huxley model is approached (FitzHugh, 1955). In the present case, the difference, $I_{STIM} - I_{K(Ca)}$, acts as an 'effective ramp stimulus' on the primary spiking currents, I_{Na} and I_K. This is so because $I_{K(Ca)}$ declines throughout each interspike interval as the excess cytoplasmic Ca^{2+} is sequestered. Ca-influx during the subsequent action potential re-activates $I_{K(Ca)}$, and therewith resets the 'effective ramp stimulus' (the gating of $I_{K(Ca)}$ is given in Computational Procedure). It is perhaps worth noting that, although the 'ringing' is an *active* gating response of I_{Na} and I_K, the response is subthreshold and therefore remains local (i.e., near the site of impulse-initiation in multi-compartment simulations). Thus, the 'ringing' does *not* propagate with the subsequently traveling action potentials on the axon, which are more abruptly initiated by the tri-phasic electrotonic current-pulse that 'sweeps' along the axon with each action potential.

The 'ringing' is an expression of the high frequency oscillator characteristic of the Hodgkin-Huxley model, and is a direct consequence of the model's early K-channel activation gating (see Results). Note in the right hand panels of Fig. 5, that $G_K > G_{Na}$ throughout the interspike interval for both Hodgkin-Huxley models, in contrast to the RGC model for which $G_K < G_{Na}$, and which does *not* 'ring.' Note also that the magnitude-scale of the ionic conductances in the interspike interval, G_K and G_{Na}, is two orders of magnitude larger for the Hodgkin-Huxley models than for the RGC model. Finally, the compound Hodgkin-Huxley model remains highly energy-inefficient, with 86.4 % of Na^+ ions entering the neuron after the peak of the action potential (at 37° C).

A possible molecular gating-difference between the squid axon and retinal ganglion cells

In assessing the Hodgkin-Huxley model for mammalian excitation, it was necessary to bridge the wide temperature span between the standard 6.3° C of the Hodgkin-Huxley model, and the mammalian 37° C (standard for the RGC model). It was noted in Results that the gating of retinal ganglion cells involves two distinct Q10 behaviors in neighboring temperature ranges (uniformly *constant* Q10 = 1.9 to 1.95 for T > 23° C; *increasing* Q10 for T < 23° C; see Fig. 4A).

This empirical Q10-behavior of RGC gating is consistent with an earlier study of K-channel activation-gating in rat skeletal muscle, which shows Q10 = 2 for the range $30° \leq T \leq 38°$ C, and Q10 = 6 in the range $1° < T < 10°$ C (Beam and Donaldson, 1983). Significantly, perhaps, this relatively high Q10 = 6 occurs in conjunction with a time delay in activation-gating. Such an emerging time delay can be an indication of additional kinetic steps that were previously hidden, as was proposed by Cole and Moore (1960) in an analogous situation. The hidden steps *here* become exposed by low temperature (in place of the pre-hyperpolarization for the "Cole-Moore shift"). As pointed out in Results, a substantial temperature range of constant Q10 (T > 23° C), with its neighboring lower temperature range of increasing Q10 also suggests that two distinct processes are simultaneously active in mammalian channel gating. Thus, the process of high Q10 (= 6 to 8; see Fig. 4A) is electro-physiologically detected because it becomes rate-limiting at low temperatures (specifically for T < 23° C), but speeds up sufficiently at high temperatures, so as to be masked (i.e., electro-physiologically hidden) by the then slower process of low Q10 (= 2).

It is remarkable that the Hodgkin-Huxley model and RGCs share a *common* Q10 (= 1.9 to 2) for the partial temperature range of T > 23° C (Fig. 4A), as determined from impulse-matches throughout the range of 23° to 37° C. This suggests the existence of a common gating process for the two preparations. This common process appears to be the *only* process in squid axon gating, because virtually the same Q10 (= 2) yields also a match with the experimental squid axon at 6.3° C, and thus extends the applicable range of Q10 = 2 for the squid axon down to 6.3° C. Because Q10 = 2 is also typical for enzyme-kinetics, this common process could be restricted to conformational changes in a single protein molecule (e.g., the Na-channel of *electroplax* sequenced by Noda et al., 1984). The second process – the one associated with the high Q10 in RGC gating – appears to be absent in squid axon gating.

Antibody or in-situ hybridization studies of sodium channels have shown sub-types Nav 1.1, 1.2, 1.3 and 1.6 in the retinal ganglion cell layer (Caldwell et al., 2000; Craner et al., 2003). The potassium channel subunits Kv 1.1 – 1.6 have also been reported to hybridize to ganglion cells (Hötje et al., 2007). It is possible that the kinetic differences exhibited by these channel sub-types are associated with the *additional* gating steps of high Q10, which could be in the nature of changing the phosphorylation state (Hidaka and Ishida, 1998), or reconfiguring polypeptide channel-subunits (Hanlon and Wallace, 2002; cf also Tiwari and Sikdar, 1999), i.e., processes whose rates may be strongly temperature-dependent. One may speculate that one (or more) of these *additional* processes are the molecular basis of the differences in the two models' rate constants. Because of their slow rates at low temperatures, such processes are likely to be detrimental to excitation in the cold environment of the squid, and are therefore absent in the squid axon. Their absence could be the cause of the early onset of K-activation gating in the squid giant axon, leading to the functional differences between the RGC model (encoder), and the Hodgkin-Huxley model (oscillator). One may speculate finally, that the additional gating process(es) – whose speed (rate) is no longer a hindrance above room temperature – evolved because of the need for highly flexible impulse encoding in mammalian central neurons, as well as the desirability of energy-efficient channel gating (Attwell and Laughlin, 2001).

4. COMPUTATIONAL PROCEDURE

Numerical integration of the basic gating kinetic equations was carried out using the Runge-Kutta method with variable integration step. The error criterion: a maximum allowable difference of < 0.01 % in all variables of state (m, h, n, V, dV/dt) when the integration steps are increased by a factor of 10.

Gating rate constants

All rate constants and parameters listed under "Hodgkin-Huxley Model" are original, except modified to modern convention. The RGC model rate constants involve two principal types of modification of Hodgkin and Huxley (1952):

1. Voltage-shifts (i.e., changes in the numerical quantities that are added directly to the variable "V" in the equations below).
2. Channel-specific increases in the overall gating rates (underlined coefficients of the rate constants).

There is, in addition, a small reduction in the steepness of the voltage-rate-of-change in Na-activation gating (see Fig. 1B, and β_m (V) below).

The (underlined) coefficients listed under "RGC Model" yield 'matching' action potentials (duration and amplitude) with the Hodgkin-Huxley model at 6.3° C (these correspond to RGC

data at 13.9° C, see Results). The steady-state fractions of open channels, and the activation time constants of the two models are compared in Figs. 1B and 1C, respectively.

	Hodgkin-Huxley Model		RGC Model	
	Na-activation:			
α_m (V):	$-\underline{0.1}(V + 35) / [\exp(-0.1(V + 35)) - 1]$		$-\underline{0.3753}(V + 35) / [\exp(-0.1(V + 35)) - 1]$	
β_m (V):	$\underline{4} \exp[-(V + 60) / 18]$		$\underline{12.51} \exp[-(V + 60) / 20]$	
	Na-inactivation:			
α_h (V):	$\underline{0.07} \exp[-(V + 60) / 20]$		$\underline{0.2502} \exp[-(V + 52) / 20]$	
β_h (V):	$\underline{1} / [1 + \exp(-0.1 (V + 30))]$		$\underline{3.753} / [1 + \exp(-0.1 (V + 22))]$	
	K-activation (delayed rectifier):			
α_n (V):	$-\underline{0.01}(V + 50) / [\exp(-0.1(V + 50)) - 1]$		$-\underline{0.01319}(V + 37) / [\exp(-0.1(V + 37)) - 1]$	
β_n (V):	$\underline{0.125} \exp[-(V + 60) / 80]$		$\underline{0.2638} \exp[-(V + 47) / 80]$	
	Ca-activation (H-type):			
α_c (V):	$-\underline{0.05}(V + 13) / [\exp(-0.1(V + 13)) - 1]$ *		$-\underline{0.1877}(V + 13) / [\exp(-0.1(V + 13)) - 1]$	
β_c (V):	$\underline{1.667} \exp[-(V + 38) / 18]$ *		$\underline{6.256} \exp[-(V + 38) / 18]$	
	Open Channel Conductances [Reversal Potentials]			
G_{Na} [V_{Na}]:	120 mS / cm^2	[+ 55 mV]	19.425 mS / cm^2	[+ 54.96 mV]
G_K [V_K]:	36 mS / cm^2	[− 72 mV]	7.286 mS / cm^2	[− 91.90 mV]
G_{Ca} [V_{Ca}]:	3.305 mS / cm^2	[variable] *	0.535 mS / cm^2	[variable]
$G_{K(Ca)}$ [$V_{K(Ca)}$]:	0.247 mS / cm^2	[− 72 mV] *	0.050 mS / cm^2	[− 91.90 mV]

* The Ca-system (I_{Ca} and $I_{K(Ca)}$) is not a part of the Hodgkin-Huxley model; it is sometimes added here to that model to test its effects in model comparisons.

The Ca-activated K-current, $I_{K(Ca)}$, is gated according to:

$$g_{K(Ca)} = G_{K(Ca)} [X^2/(1+X^2)],$$

where the dimensionless $X = [Ca^{2+}]_i / Ca_{diss}$, with $Ca_{diss} = 10^{-3}$ (Ca-dissociation constant in milliMolar), and variable $[Ca^{2+}]_i$ (cytoplasmic Ca-concentration in the same units), which is determined by the equation (Fohlmeister and Miller, 1997a):

$$d[Ca^{2+}]_i/dt = -3I_{Ca}/2Fr - ([Ca^{2+}]_i - [Ca^{2+}]_{res})/\tau_{Ca},$$

where F = Faraday, r = 15 μm (cell radius), τ_{Ca} = 50 ms (Ca-sequester time), and $[Ca^{2+}]_{res} = 10^{-4}$ mM (residual cytoplasmic Ca-concentration). The Ca-reversal potential varies according to:

$$V_{Ca} = RT/2F \ \ln\left\{1.8mM/[Ca^{2+}]_i(t)\right\}.$$

Conversions for mammalian temperatures (37° C)

To obtain the gating rate constants for 37° C, apply Q10 = 2 to the above underlined coefficients for both models. This is equivalent to multiplying the underlined coefficients by the factor =

$2^{(T-6.3)/10}$ (= 8.398 for T = 37° C). The voltage-dependence of the rate constants remains temperature-independent.

For the RGC model, apply also the *conductance* Q10 = 1.47 to the above listed G_{Na}, G_{K}, G_{Ca} and $G_{K(Ca)}$ (multiplicative factor = 3.263 for T = 37° C; cf Milburn et al., 1995; Rodriguez et al., 1998). For the Hodgkin-Huxley model, apply the *conductance* Q10 = 1.25 (multiplicative factor = 1.984 for T = 37° C). These Q10s are chosen to maintain model matches in impulse-amplitude at both 6.3° C and 37° C.

The reversal (Nernst) potentials were temperature-adjusted by applying the factor: (273 + T)/(273 + 6.3) to the values listed above; this factor = 1.11 for T = 37° C. Fig. 1A gives the action potential and associated membrane currents of the RGC model at 37° C.

ACKNOWLEDGMENTS

Thanks to the Minnesota Supercomputer Institute for access to computing facilities for this study. This research was supported by NIH grant R01EY012833-06 to R. F. Miller.

REFERENCES

Attwell D, Laughlin SB. An energy budget for signaling in the gray matter of the brain. J. Cereb Blood Flow Metab 2001;21:1133–1145. [PubMed: 11598490]

Beam KG, Donaldson PL. A quantitative study of potassium channel kinetics in rat skeletal muscle from 1 to 37 degrees C. J. Gen. Physiol 1983;81:485–512. [PubMed: 6304231]

Caldwell JH, Schaller KL, Lasher RS, Peles E, Levinson SR. Sodium channel Na(v)1.6 is localized at nodes of ranvier, dendrites, and synapses. Proc. Natl. Acad. Sci. U.S.A 2000;97:5616–5620. [PubMed: 10779552]

Cole KS, Moore JW. Potassium ion current in the squid giant axon: dynamic characteristic. Biophys. J 1960;1:1–14. [PubMed: 13694549]

Craner M, Lo A, Black J, Waxman S. Abnormal sodium channel distribution in optic nerve axons in a model of inflammatory demyelination. Brain 2003;126:1552–1561. [PubMed: 12805113]

FitzHugh R. Mathematical models of threshold phenomena in the nerve membrane. Bull. Math. Biophys 1955;17:257–278.

Fohlmeister JF, Adelman WJ, Poppele RE. Excitation properties of the squid axon membrane and model systems with current stimulation: Statistical evaluation and comparison. Biophys. J 1980;30:79–98. [PubMed: 7260270]

Fohlmeister JF, Coleman PA, Miller RF. Modeling the repetitive firing of retinal ganglion cells. Brain Research 1990;510:343–345. [PubMed: 2331606]

Fohlmeister JF, Miller RF. The impulse encoding mechanism of ganglion cells in the tiger salamander retina. J. Neurophysiol 1997a;78:1935–1947. [PubMed: 9325362]

Fohlmeister JF, Miller RF. Mechanisms by which cell geometry controls repetitive impulse firing in retinal ganglion cells. J. Neurophysiol 1997b;78:1948–1964. [PubMed: 9325363]

Fohlmeister JF, Cohen ED, Newman EA. Mechanisms and Distribution of Ion Channels in Retinal Ganglion Cells; Using Temperature as an Independent Variable. J. Neurophysiol. 2009(In press)

Fourcaud-Trocme N, Hansel D, van Vreeswijk C, Brunel N. How spike generation mechanisms determine the neuronal response to fluctuating inputs. J. Neurosci 2003;23:11628–11640. [PubMed: 14684865]

Hanlon MR, Wallace BA. Structure and function of voltage-dependent ion channel regulatory beta subunits. Biochemistry 2002;41(9):2886–2894. [PubMed: 11863426]

Hidaka S, Ishida AT. Voltage-gated Na+ current availability after step- and spike-shaped conditioning depolarizations of retinal ganglion cells. Pflugers Arch 1998;436:497–508. [PubMed: 9683721]

Hodgkin AL, Huxley AF. A quantitative description of membrane current and its applications to conduction and excitation in nerve. J. Physiol. (London) 1952;117:500–544. [PubMed: 12991237]

Höltje M, Brunk I, Grosse J, Beyer E, Veh RW, Bergmann M, Grosse G, Ahnert-Hilger G. Differential distribution of voltage-gated potassium channels Kv 1.1-Kv1.6 in the rat retina during development. J. Neurosci. Res 2007;85:19–33. [PubMed: 17075900]

Milburn T, Saint DA, Chung SH. The temperature dependence of the conductance of the sodium channel: implications for mechanisms of ion permeation. Receptors Channels 1995;3:201–211. [PubMed: 8821793]

Naundorf B, Wolf F, Volgushev M. Unique features of action potential initiation in cortical neurons. Nature 2006;440:1060–1063. [PubMed: 16625198]

Noda M, Shimizu S, Tanabe T, Takai T, Kayano T, Ikeda T, Takahashi H, Nakayama H, Kanaoka Y, Minamino N, Kangawa K, Matsuo H, Raftery MA, Hirose T, Inayama S, Hayashida H, Miyata T, Numa S. Primary structure of *Electrophorus electricus* sodium channel deduced from cDNA sequence. Nature 1984;312:121–127. [PubMed: 6209577]

Rodriguez BM, Sigg D, Bezanilla F. Voltage gated Shaker K^+ channels. The effect of temperature on ionic and gating currents. J. Gen. Physiol 1998;112:223–242. [PubMed: 9689029]

Tiwari JK, Sikdar SK. Temperature-dependent conformational changes in a voltage-gated potassium channel. Eur. Biophys. J 1999;28:338–345. [PubMed: 10394625]

van Rossum MC, O'Brien BJ, Smith RG. Effects of noise on the spike timing precision of retinal ganglion cells.". J. Neurophysiol 2003;89:2406–2419. [PubMed: 12740401]

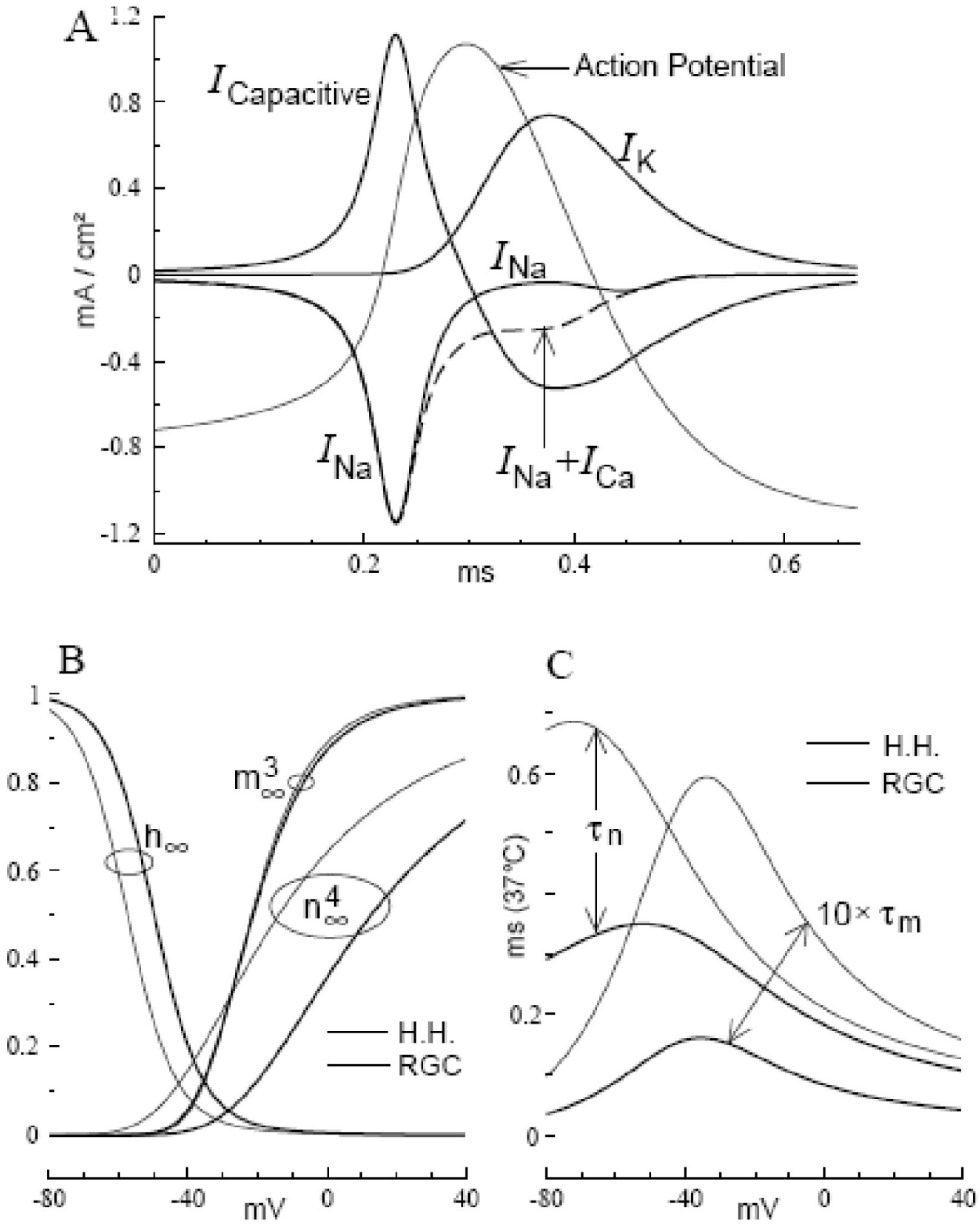

FIGURE 1. Membrane currents of the RGC model action potential at 37° C

A. The ionic currents I_{Na} and I_K are restricted to the regenerative and falling phases of the action potential, respectively. **B.** Steady-state fractions of open channel-gates as functions of membrane potential: m_∞^3 (V) [Na-activation], h_∞ (V) [Na-inactivation], n_∞^4 (V) [K-activation], where $x_\infty(V) = \alpha_x(V) / [\alpha_x(V) + \beta_x(V)]$; x = m, h, n. Note the shift in the voltage-onset of n_∞^4 (V) from prior to m_∞^3 (V) [Hodgkin-Huxley model], to after m_∞^3 (V) [RGC model]. **C.** The activation gating time constants, $\tau_x(V) = 1 / [\alpha_x(V) + \beta_x(V)]$ are compared for the two models. Note that, in general, gating is faster in the RGC model, with a greater increase in the rate of Na-channel gating.

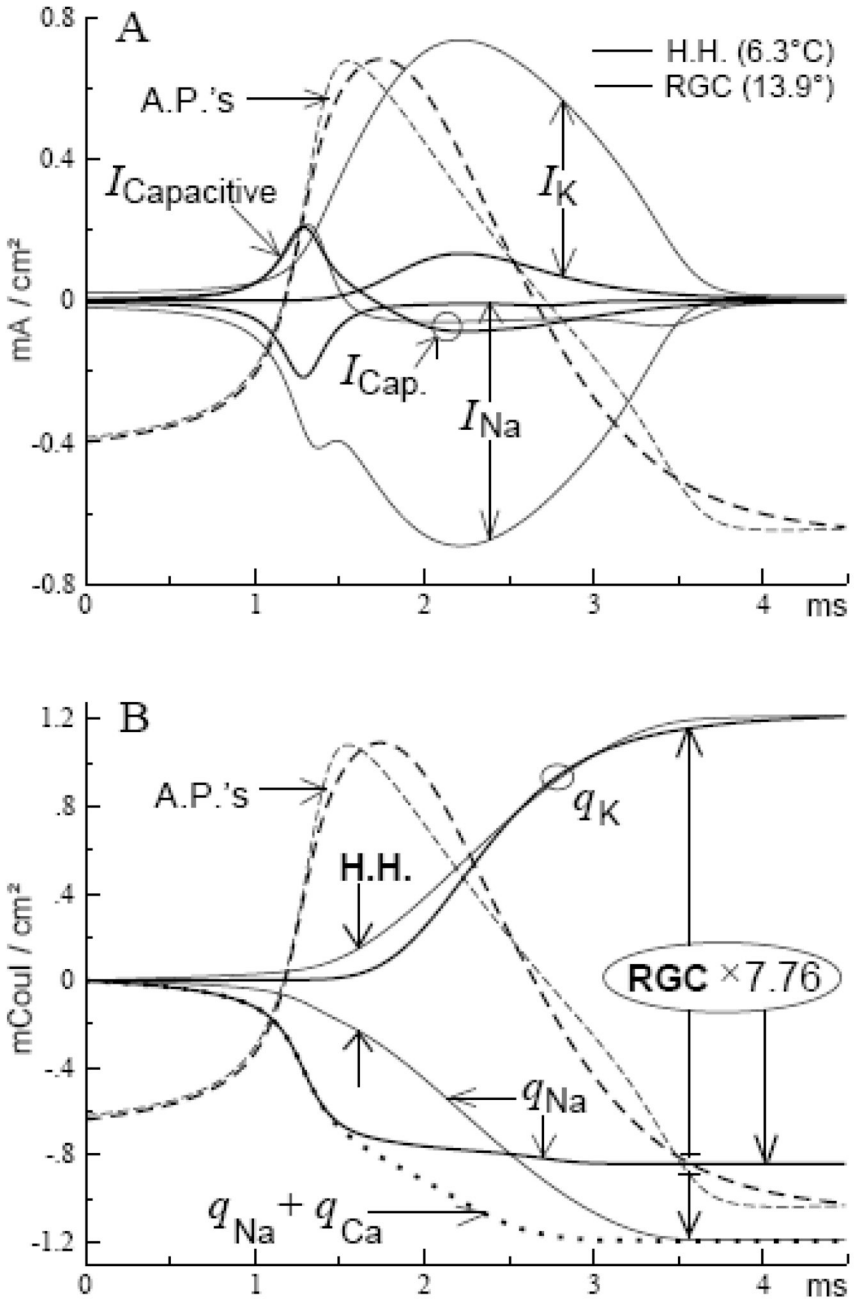

FIGURE 2. Ion transfers across the membrane during action potentials (6.3° C)

A. Membrane currents of the RGC (heavy curves), and Hodgkin-Huxley models (thin curves); the model action potentials were matched by duration and amplitude (dashed curves; see text). **B.** Accumulating totals of ionic charges (*q*) transferred across the membrane during action potentials. The final totals are greater for the Hodgkin-Huxley model by a factor of 7.76 (*expanded scale* for the RGC model). Note that the *onsets* of ion-transfer (Na^+ and K^+) are virtually simultaneous for the Hodgkin-Huxley model, but are temporally staggered for the RGC model; note also that Na^+-transfer continues throughout the falling phase of the Hodgkin-Huxley model action potential.

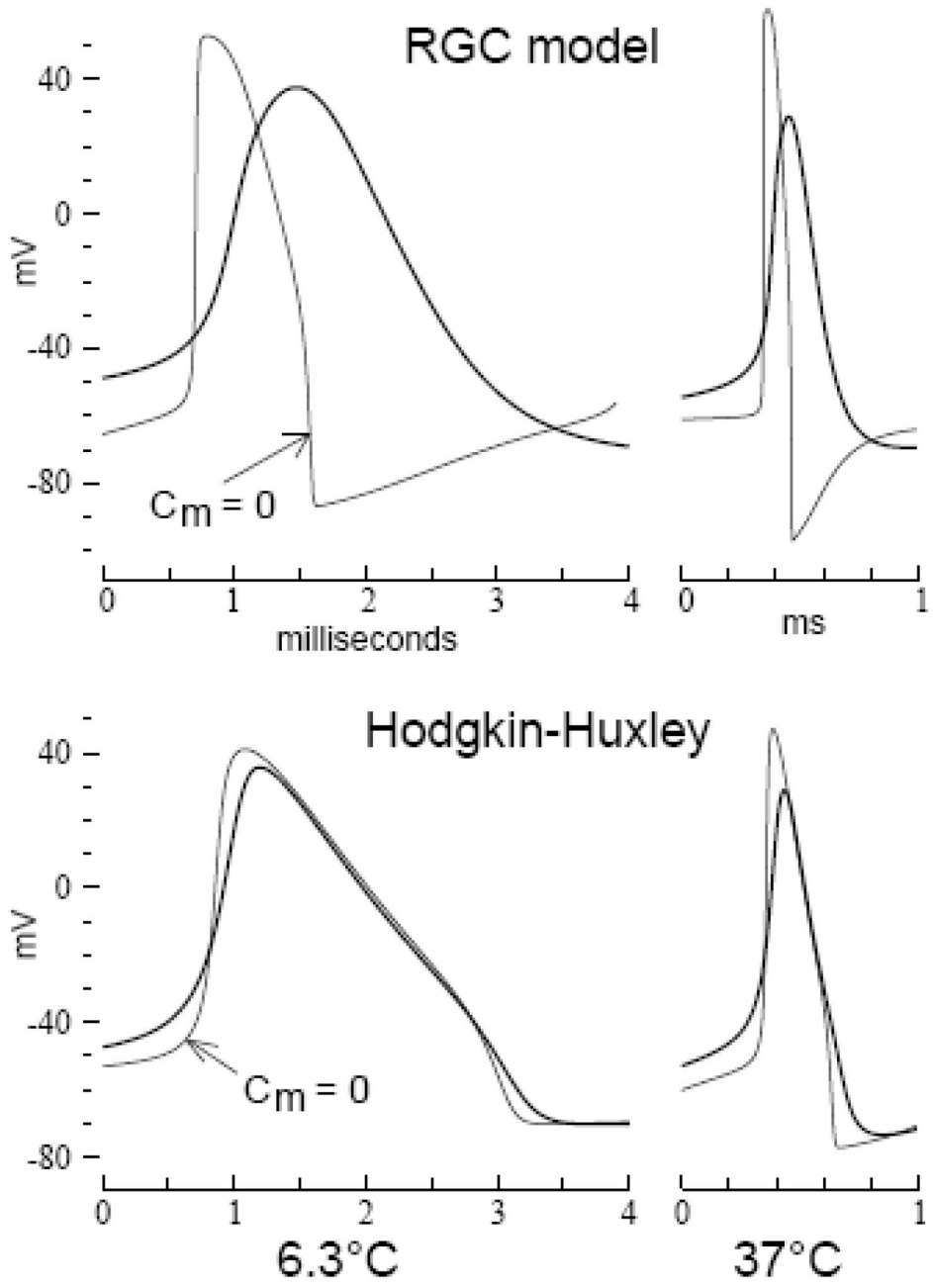

FIGURE 3. Capacitive 'smoothing' of action potentials at 6.3° and 37° C

Action potentials of the RGC and Hodgkin-Huxley models (top and bottom, respectively), in the presence and absence of membrane capacitance ("zero-C" action potentials; heavy and thin curves, respectively). Note that capacitive smoothing is strongly model-dependent, but is nearly temperature-*in*dependent (see text).

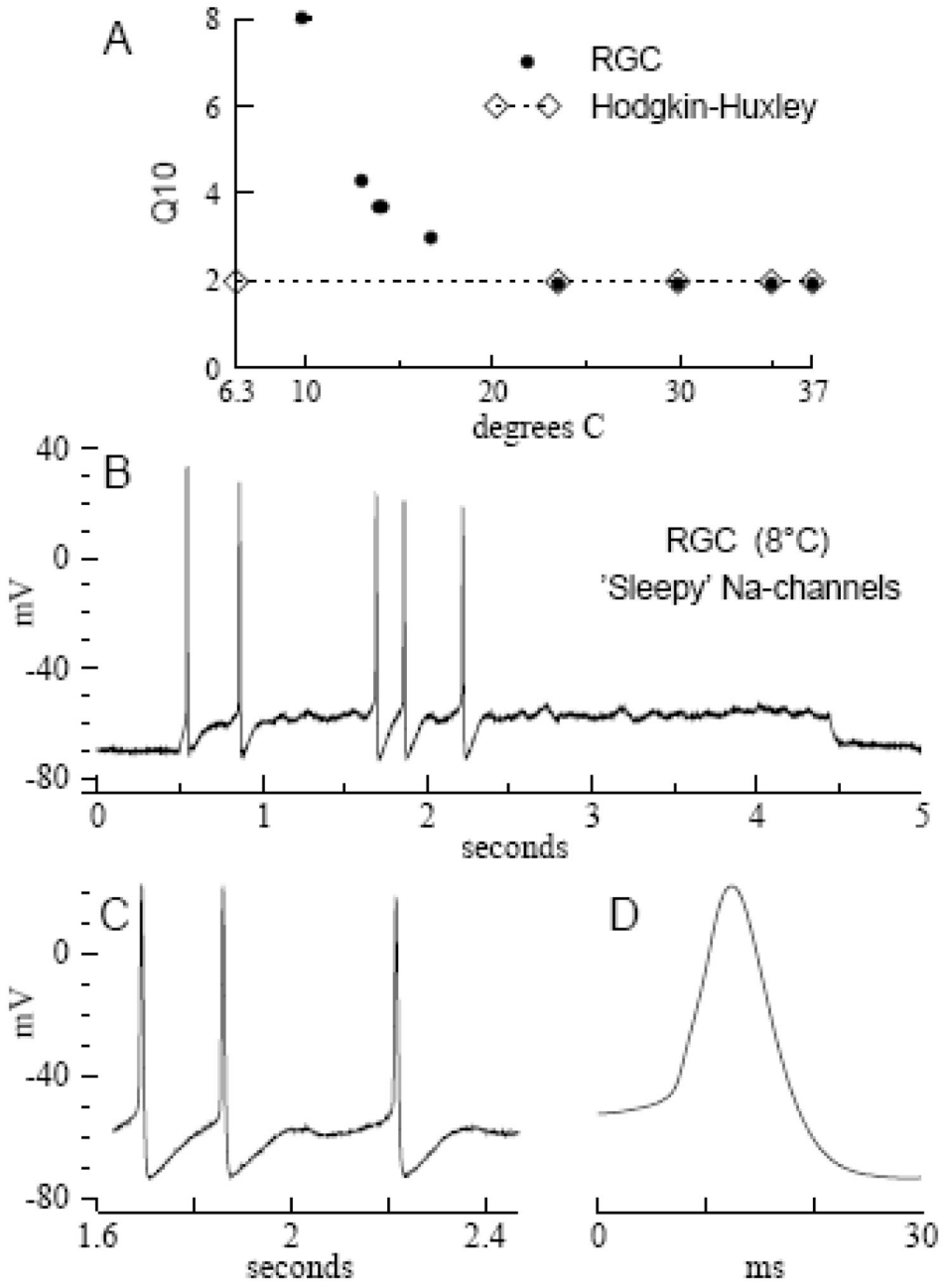

FIGURE 4. Temperature's effects on the gating kinetics

A. Gating kinetic Q10s as functions of temperature. The temperature-independent Q10 = 2 yields action potential 'matches' with the Hodgkin-Huxley model from 6.3° C through 37° C (*open diamonds connected by small dots*; see text). *Heavy dots* show the experimental Q10s of Na- and K-channel gating in rat RGCs as functions of temperature (data taken from Table 2 in Fohlmeister et al., 2009). **B.** An impulse train from a rat RGC with 'sleepy' Na-channels at 8° C (for Methods, see Fohlmeister et al., 2009). The Hodgkin-Huxley-like membrane potential oscillations, including phase-locked spiking, are absent for T > 8° C (see text). **C.** Expanded segment of the impulse train in B., showing oscillator regularity and apparent gating

kinetic control of the interspike trajectory (cf. Fig. 5, central records). **D.** A single ‘sleepy’ action potential of long duration from the impulse train in B (see text).

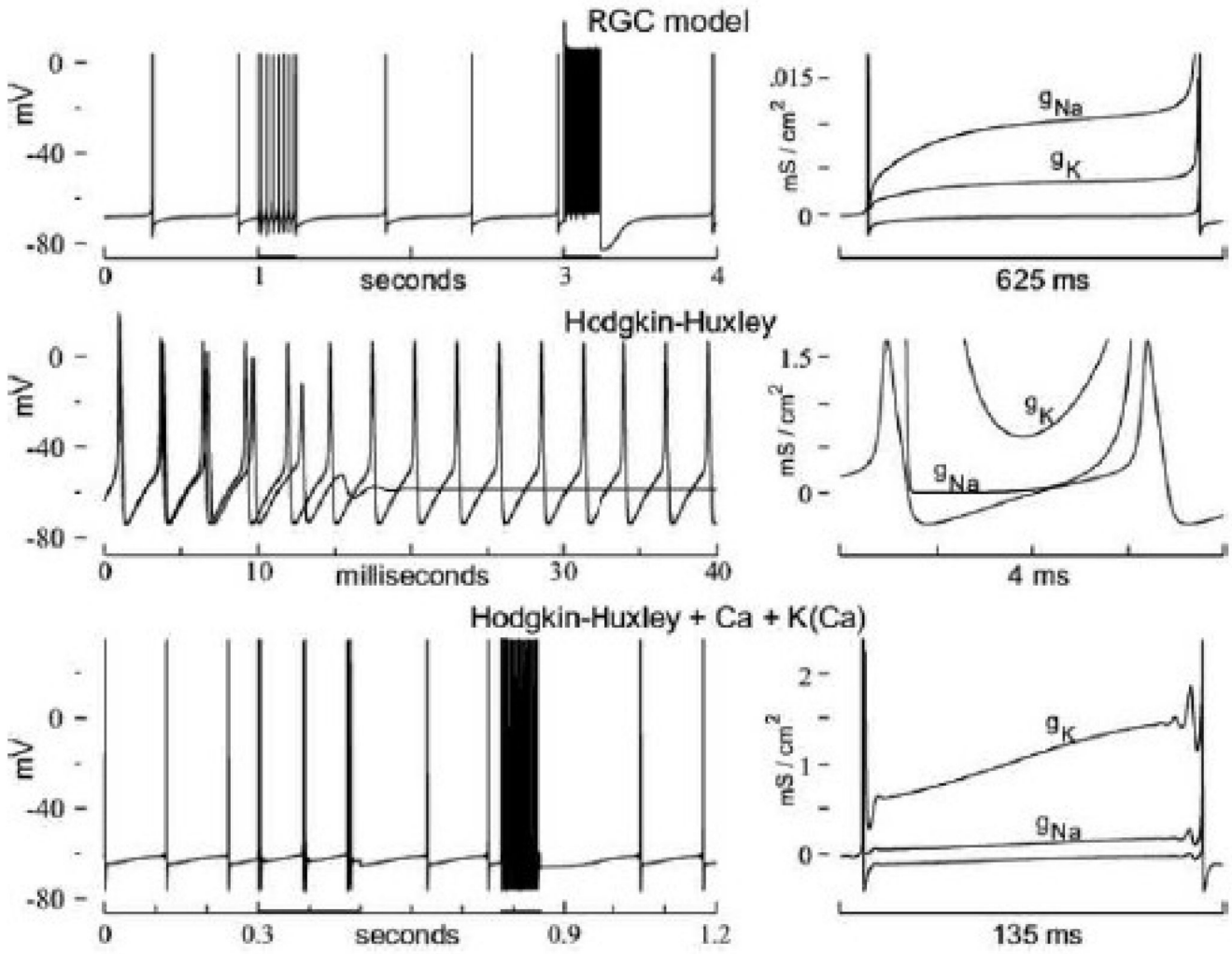

FIGURE 5. Repetitive firing at 37° C

Top: Very low frequency repetitive firing by the RGC model (1.78 impulses / sec; I_{STIM} = 0.0165 μA/cm^2). The 4 seconds record is twice interrupted by periods of larger I_{STIM} = 0.75 μA/cm^2 (at 1 second) and 50.0 μA/cm^2 (at 3 seconds), yielding 27.24 and 1,015 impulses / sec, respectively. **Center:** Two (superposed) impulse trains generated by the Hodgkin-Huxley model with I_{STIM} = 21 μA/cm^2 (dashed), and 21.5 μA/cm^2 (continuous curve). Note that I_{STIM} = 21.5 μA/cm^2 is just above threshold for tonic repetitive firing, yielding the model's lowest impulse frequency = 367 impulses / sec (at 37° C; see text). **Bottom:** Low frequency repetitive firing by the Hodgkin-Huxley model plus $I_{K(Ca)}$ and I_{Ca}, and with the threshold reduced to just above spontaneous firing (i.e., increased G_{Na} = 384.4 mS/cm^2). Note the two periods of larger stimuli during which impulse-doublets, and high frequency repetitive firing occur (details of the F/I properties are given in the text). **Right panels:** Membrane conductances, g Na (dashed) and g_K (dot-dash), during a single interspike interval of the low frequency firing records on the left. Note the model-specific order, and model-specific magnitude scales of g_{Na} and g_K (see text).